



Supplement of

Cold spells induced by slow-moving and amplified large-scale ridge and trough

Morteza Babaei et al.

Correspondence to: Morteza Babaei (morteza.babaei@uit.no)

The copyright of individual parts of the supplement might differ from the article licence.

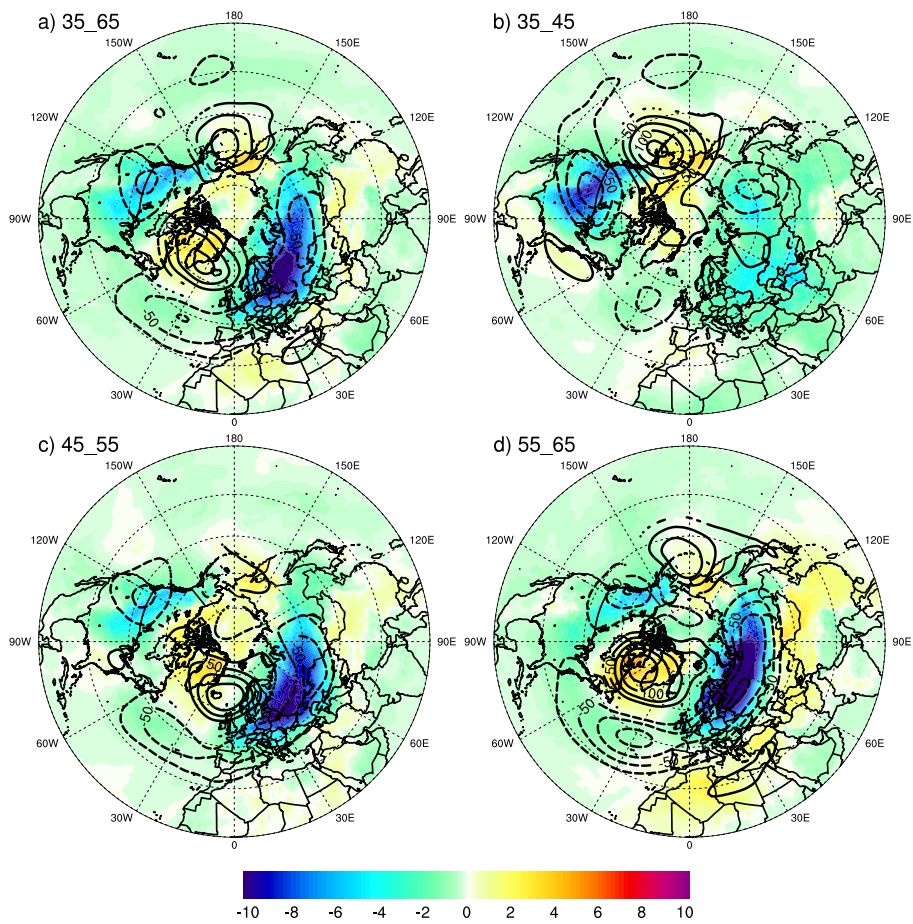


Figure S1. The composite of the geopotential height anomaly of cold extreme days given by the top 1 % of the mid-latitude extreme (MEX; Riboldi et al., 2020) index over land relative to climatology (m) at 500 hPa (lines; only significant at the 95 % confidence level), and the corresponding composite of 2-meter daily temperature anomaly relative to climatology (K; colors) at the latitude band of a) 35–65° N, b) 35–45° N, c) 45–55° N, and d) 55–65° N.

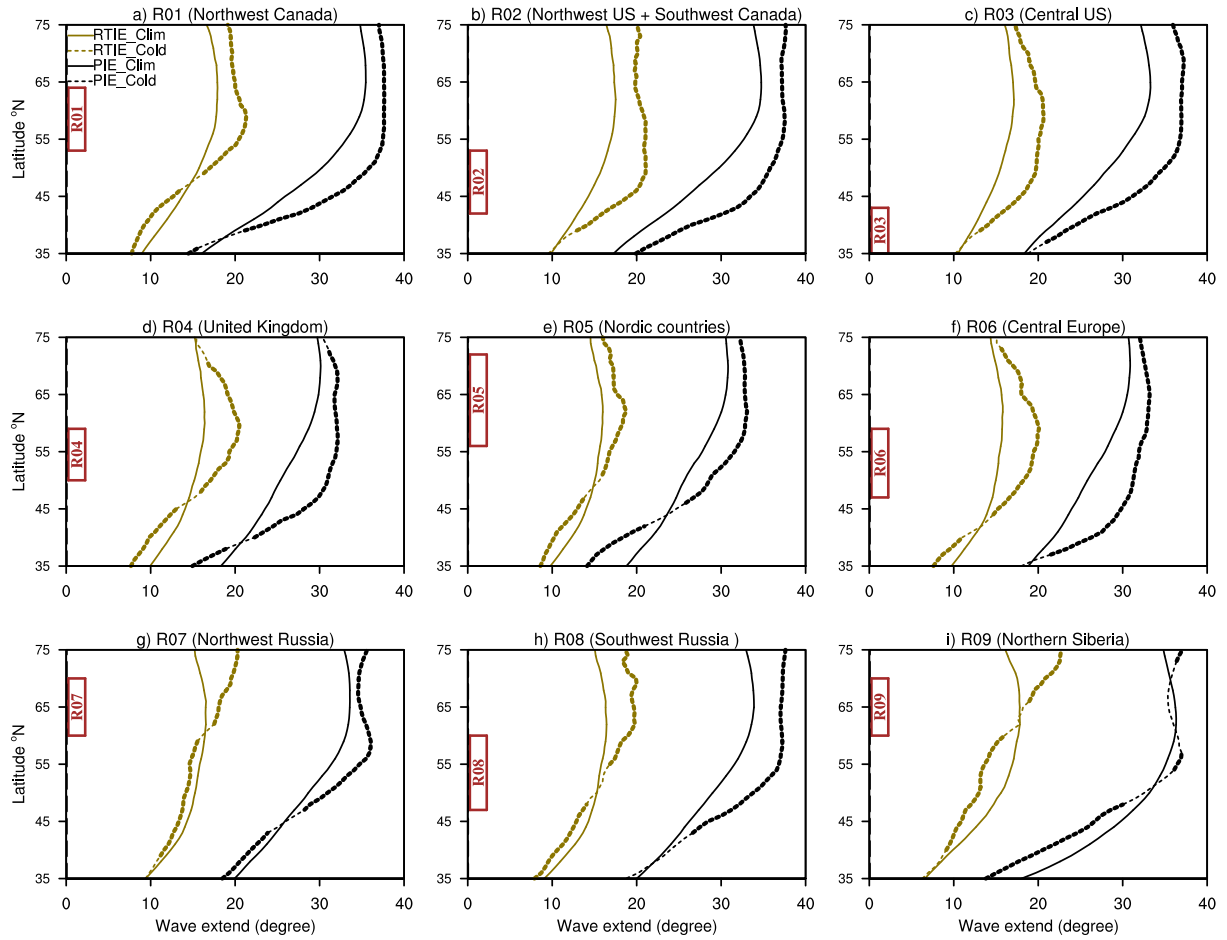


Figure S2. Climatology (solid lines) and a composite of cold spells (dashed lines) for the latitude isohypse extend (PIE; blacks) and the ridge-trough isohypse extend (RTIE; golds) of the Z1-5 at 300 hPa. See the wave metrics section for detailed information about the calculation of these metrics. Bold dashed lines indicate the significance of the cold spell composite at the 95 % confidence level. a) Northwest Canada; b) Northwest US and Southwest Canada; c) Central US; d) British Isles; e) Scandinavia; f) Europe; g) Northwest Russia; h) Southwest Russia; and i) Northern Siberia.

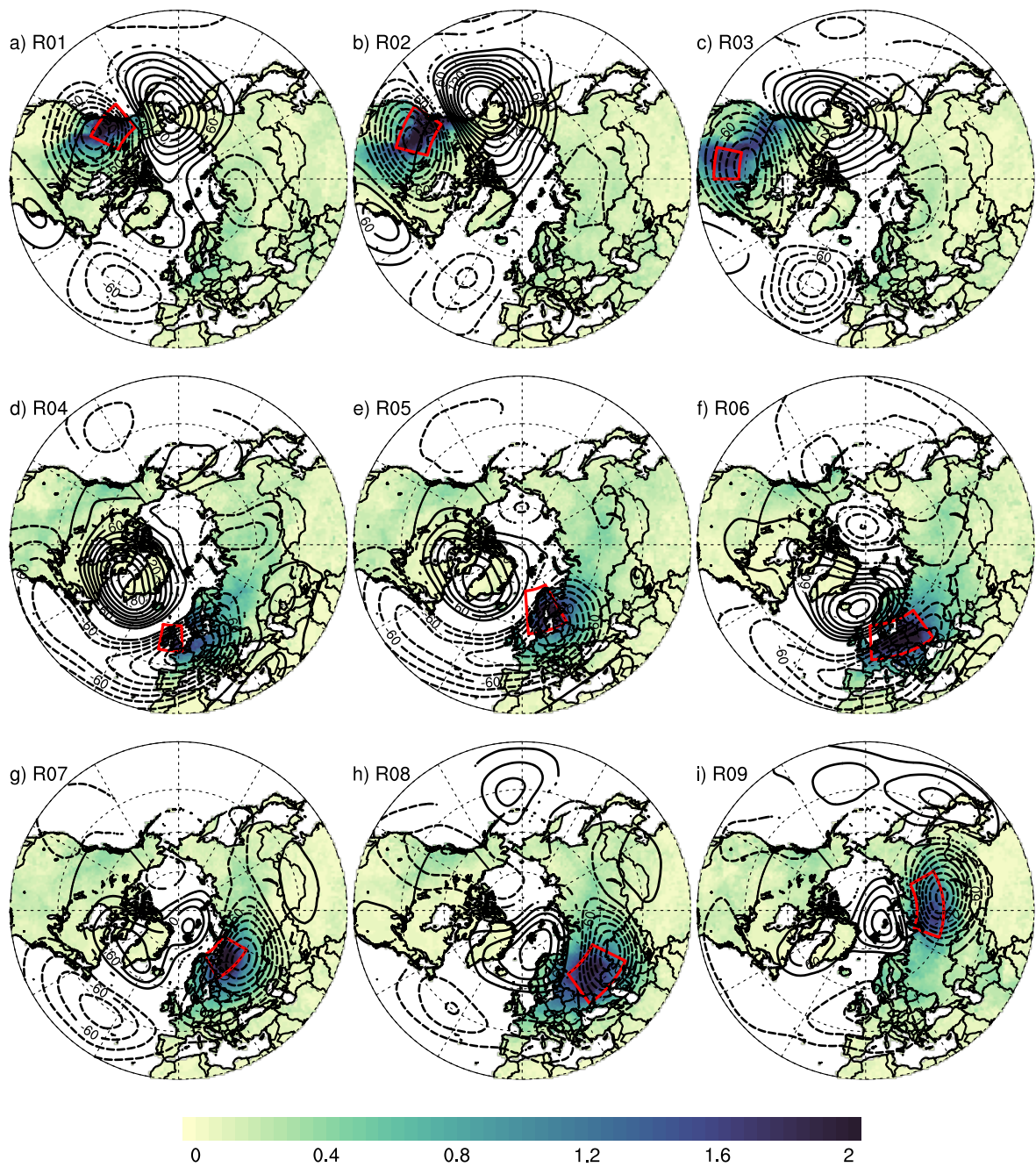


Figure S3. Similar to Fig. 1 in the main text, but for days when a cold spell is encountered in at least 50 % of land grid points in each region. The red boxes show the location of cold spells. The regions depicted here correspond to those in Fig. S2.

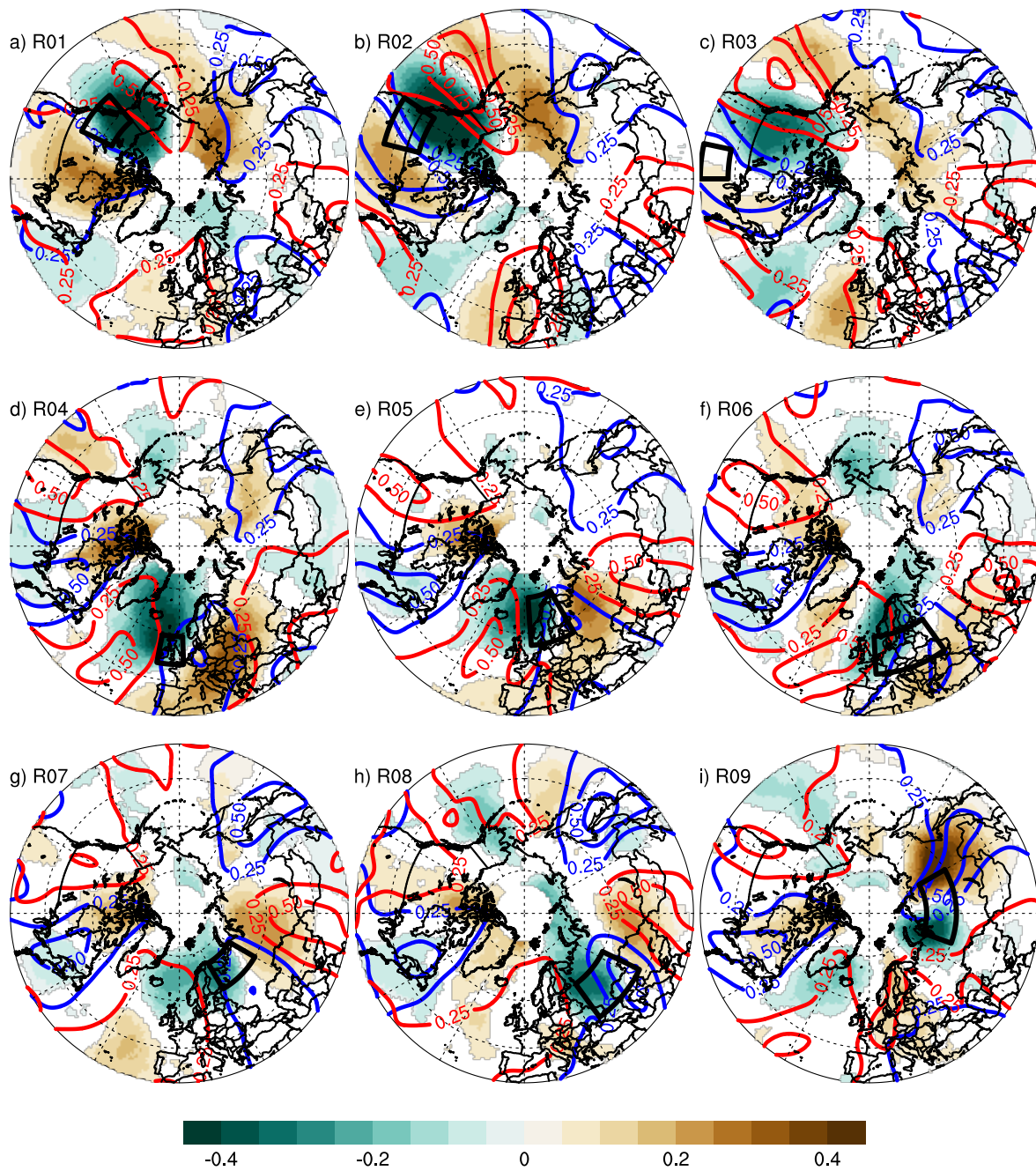


Figure S4. Composite of meridional circulation index (MCI; Francis and Vavrus, 2015) anomaly relative to climatology at 300 hPa during cold spells over each region (shadings; only significant patterns at the 95 % confidence level are shown); and the probability of ridges (solid red contours) and troughs (solid blue contours) positions in percentage at 300 hPa during cold spells over each region. The MCI shows the meridionality of flow by measuring the ratio of the meridional wind velocity to the total horizontal wind speed. The black box in each plot shows the location of the cold spell region. The regions depicted here correspond to those in Fig. S2. A Gaussian function, using a weighted running average over twelve degrees in latitude and over an equal distance in longitude, is used to smooth the probabilities.

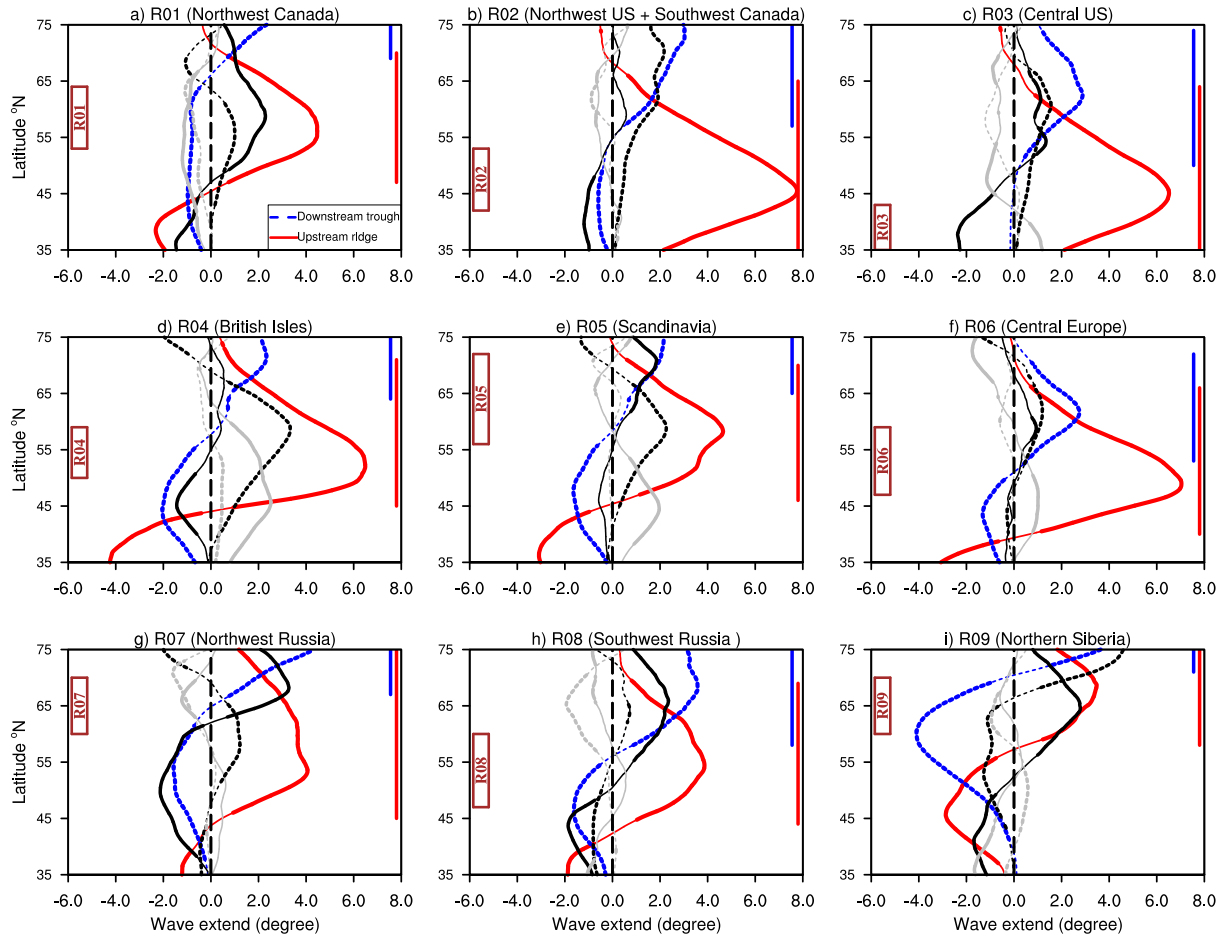


Figure S5. Composite of meridional wave amplitude anomaly (degree) relative to climatology during cold spells at 500 hPa. Red and blue lines are showing the composite of the upstream ridge and the downstream trough in the vicinity of each cold spell region, respectively. The black lines represent the ridges and troughs located at an intermediate distance, and the gray lines at the farthest distances from the cold spell region. Solid and dashed lines are for ridges and troughs, respectively. These ridges and troughs are the same as those in the wave metrics section, but here they are shown in relation to the cold spell's location. Thick solid and dashed lines indicate difference from climatology at a 95 % significance level. The regions depicted here correspond to those in Fig. S2. Vertical lines on the right side of each plot show the latitude range used for Fig. S7 and Fig. 9. These lines show the latitude range of the significant amplitude anomaly for the upstream ridge and downstream trough in the vicinity of the cold spell region. A four-degree running average is used to smooth the lines.

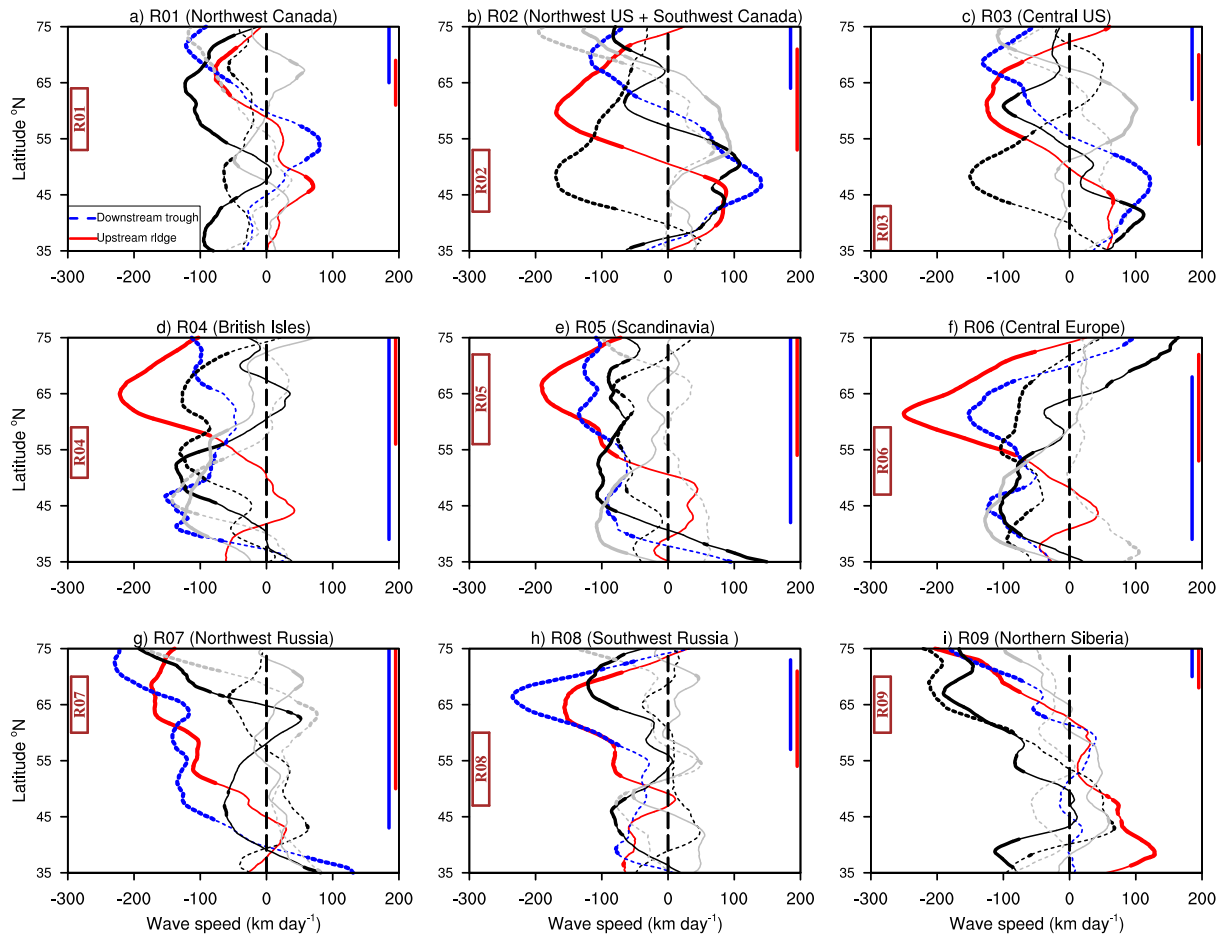


Figure S6. Similar to Fig. S5 but for wave speed (km d^{-1}) at 500 hPa.

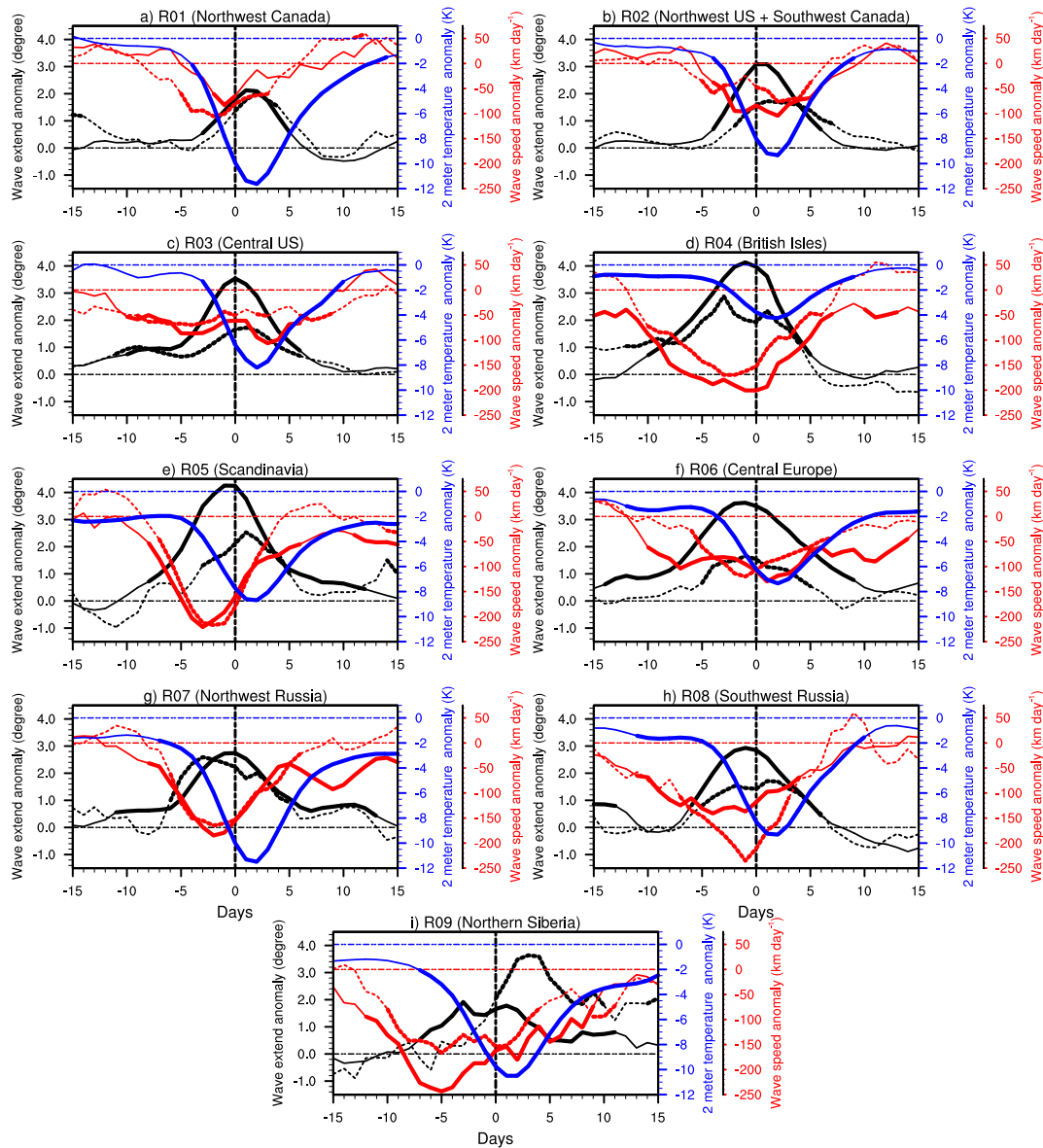


Figure S7. Composites of anomalies relative to climatology of 2-meter temperature, and ridge and trough speed and amplitude during cold spells as a function of time lag for all study regions. The lag zero (zero on the x-axis) is the day that 30 % of the land experiences a cold spell. Blue line is the composite of temperature anomalies averaged over the whole study region. Black and red lines are the composites of ridge and trough amplitude and speed anomalies at 300 hPa, respectively. The upstream ridge and the downstream trough in the vicinity of the cold-spell location are shown by solid and dashed lines, respectively. The latitude bands with a significant positive wave amplitude anomaly and a negative wave speed anomaly are averaged for each cold spell region (indicated by the vertical solid lines on the right side of Figs. S5 and S6). Bolded solid and bolded dashed lines indicate the difference to climatology significant on a 95 % level. The regions depicted here correspond to those in Fig. S2. A five-day running average is used to smooth the lines.

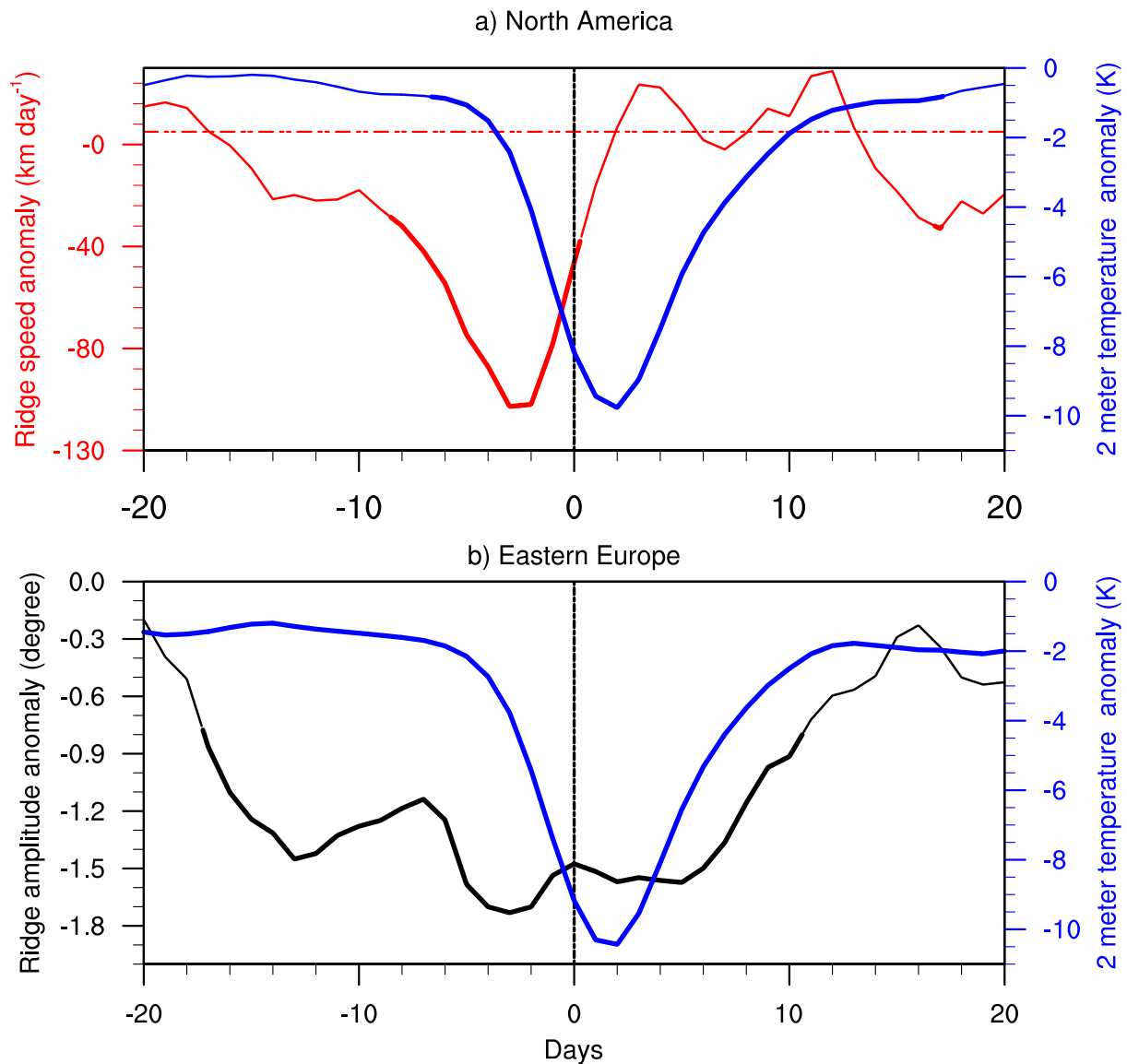


Figure S8. Composites of anomalies relative to climatology for 2-meter temperature, ridge speed, and amplitude during cold spells over a) North America (R01, R02, and R03) and b) Eastern Europe (R07 and R08), as a function of time lag. The lag zero (zero on the x-axis) is the day that 30 % of the land in each region experiences a cold spell. The blue line shows the composite of temperature anomalies averaged across each study region. The black and red lines represent the composites of the upstream ridge’s amplitude and speed anomalies, respectively, in the vicinity of the cold-spell location. A five-day running average is used to smooth the lines. For North America, speed anomalies are calculated based on the average from 35° N to 50° N. For Eastern Europe, the amplitude anomaly is derived from the average over latitudes 35° N to 40° N. Bolded solid and bolded dashed lines indicate the difference to climatology significant on a 95 % level.

References

- Francis, J. A. and Vavrus, S. J.: Evidence for a wavier jet stream in response to rapid Arctic warming, *Environ. Res. Lett.*, 10, 014 005, <https://doi.org/10.1088/1748-9326/10/1/014005>, 2015.
- 5 Riboldi, J., Lott, F., D'Andrea, F., and Rivière, G.: On the Linkage Between Rossby Wave Phase Speed, Atmospheric Blocking, and Arctic Amplification, *Geophys. Res. Lett.*, 47, e2020GL087 796, <https://doi.org/10.1029/2020GL087796>, 2020.